

Figure 1. Study area illustrating Incline Creek, Third Creek, and Galena Creek watersheds and model domain (thick black line indicating watershed boundaries).

Burroughs, 2003]. Accurately predicting historical low-frequency responses is central to predicting future low-frequency responses in groundwater storage, discharge to streams and springs, and water-dependent biota. Integrated models that are calibrated to historical interactions of SW/GW over wet and dry periods, and are forced with future climate data over many decades, are better suited to assess how climate change might affect water resources, and in particular, groundwater resources.

1.2. Model Description

[8] GSFLOW was used to simulate all near-surface and groundwater hydrologic processes within three watersheds

of the eastern Sierra Nevada (Figures 1 and 2). GSFLOW simultaneously accounts for climatic conditions, runoff across the land surface, variably saturated subsurface flow and storage, plus connections among terrestrial systems, streams, lakes, wetlands, and groundwater. Runoff and interflow (shallow subsurface flow) cascade to receiving streams or lakes, while including effects of saturation-excess runoff caused by shallow water table conditions. GSFLOW and its precursors have been applied in several basins across the United States to simulate SW/GW interactions [e.g., Hunt *et al.*, 2008; Markstrom *et al.*, 2008; Niswonger *et al.*, 2008; Doherty and Hunt, 2009; Koch *et al.*, 2011].

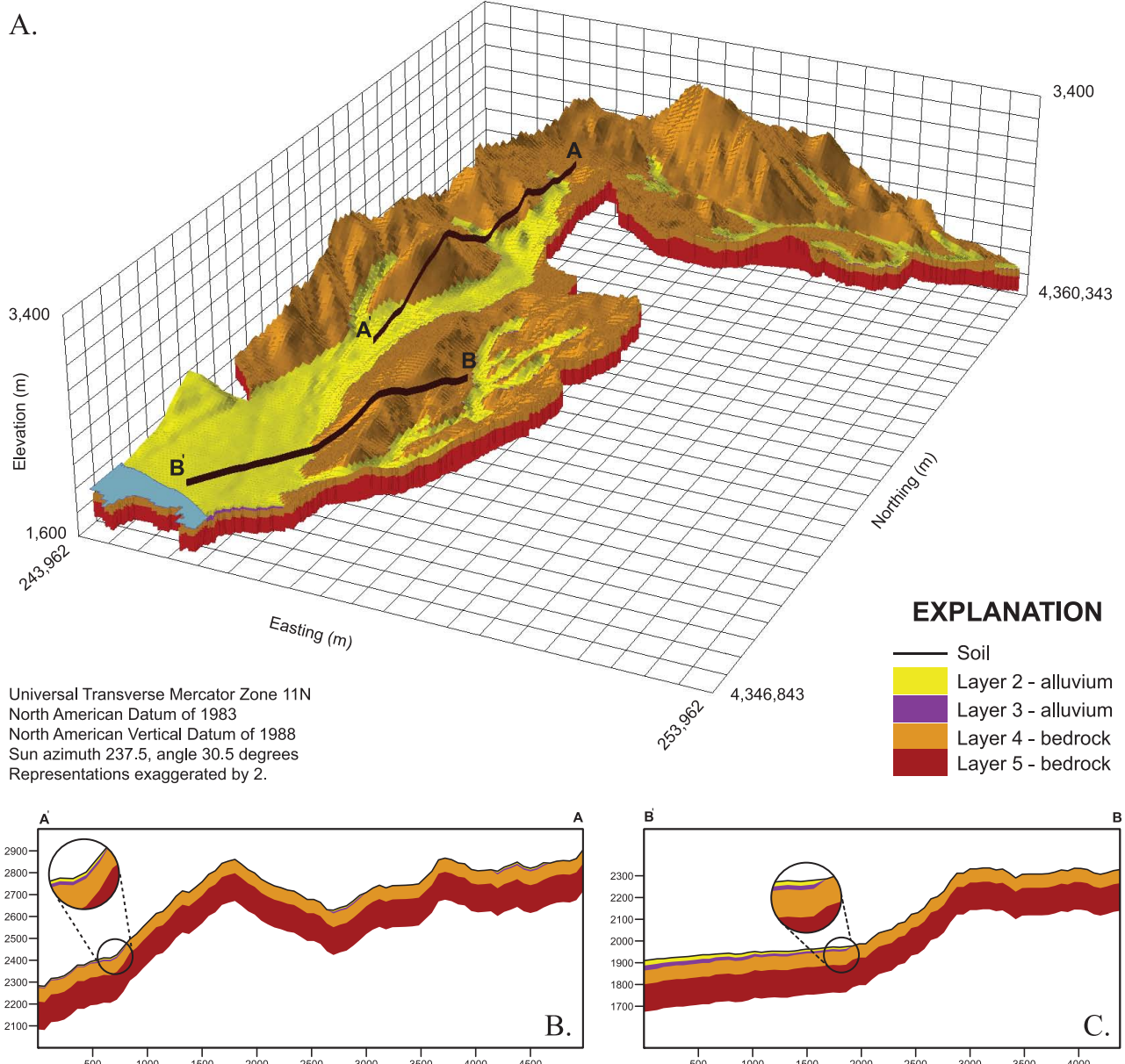


Figure 2. Three dimensional and cross section representation of the hydrogeologic framework model illustrating vertical and horizontal model discretization and hydrogeologic units.

[9] GSFLOW is the integration of the Precipitation Runoff Modeling System (PRMS) and the Modular Groundwater Flow model (MODFLOW). Integration of PRMS and MODFLOW was facilitated by an implicit iterative coupling approach using the Newton linearization method [Niswonger *et al.*, 2011]. Markstrom *et al.* [2008] and Niswonger *et al.* [2011] provide a complete description of GSFLOW and its theory, and only a broad description is provided herein. PRMS is a modular deterministic, distributed-parameter, physical-process watershed model used to simulate precipitation, climate, and land use on watershed response [Leavesley *et al.*, 1983]. PRMS simulates snowpack processes using a distributed two-layered system that is maintained and modified on both a water equivalent basis and as a dynamic heat reservoir. PRMS simulates snowmelt- and rain-generated runoff in a fully distributed sense,

where runoff can cascade among four neighboring surface grid cells, reinfiltrate, or flow to a stream. The soil zone is represented by coupled continuity equations with storages that represent different components of soil porosity (i.e., dead-end versus kinematic and macropore porosity), conceptualized in PRMS as the preferential, gravity, and capillary reservoirs. Water in the soil zone can percolate into the deeper unsaturated zone (MODFLOW), flow horizontally to a receiving grid cell or stream, or evapotranspire to the atmosphere. In areas where the water table is above the base of the soil zone, groundwater can seep into the soil zone. Additionally, groundwater discharge occurs to the surface in areas where groundwater heads are above land surface.

[10] ET is derived from the vegetation canopy and land surface (sublimation from the snowpack and evaporation

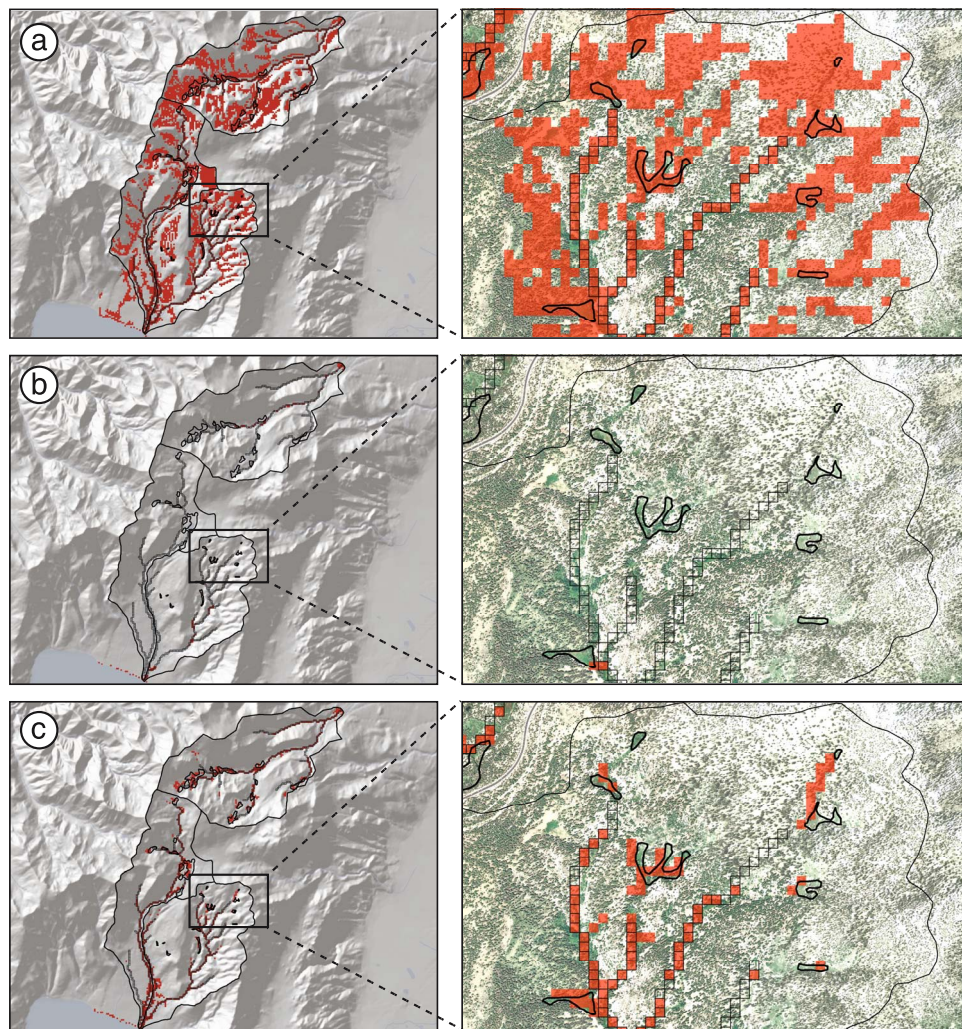


Figure 3. Spatial distribution of groundwater heads within 1 m of land surface shown as red-transparent grid cells where the hydraulic conductivity was varied by (a) a factor of 0.1 lower than calibrated values for all layers, (b) a factor of 10 greater than calibrated values for all layers, and (c) calibrated values for all layers. Black hollow grid cells are specified stream cells, and thick black polygons illustrate mapped springs and wetlands. The optimally calibrated case (Figure 3c) illustrates that the water table intersects the land surface in areas that coincide with mapped streams, springs, and wetlands.

evident that the model underpredicts heads in the upland areas and does not provide shallow groundwater levels around springs, wetlands, and perennial streams. Clearly, the calibrated K distribution provides the most accurate representation of wetland, spring, and perennial stream areas. Figure 4 shows simulated versus observed heads in wells, and land-surface elevations for spring and wetland areas. The 1-to-1 plot (Figure 4a) shows that the model simulates the head distribution accurately over a wide range in head values, with RMSE and normalized RMSE values of 3.2 m and 0.4%, respectively. A small normalized RMSE (i.e., RMSE/total head loss) as shown in this work indicates that model errors are only a small part of the overall model response [Anderson and Woessner, 1992]. The errors in simulated heads (Figure 4b) indicate that there is a slight bias in overpredicting the groundwater heads observed in wells, while underpredicting the heads in spring and wetland areas. Adding further complexity to the model to better match heads was not warranted given the model

scale and uncertainty in these observation data. Most of the wells in the study are located in steep terrain, making direct comparisons between simulated and measured heads in these wells difficult due to the grid scale. Additionally, errors in simulated wetland heads are acceptable given the subgrid variability in land surface from which the wetland observation heads were derived. Water levels in wetland areas are not always at land surface, but near land surface and within the root zone of identified wetland areas. Thus, a bias toward underpredicting the wetland heads is consistent with our conceptualization of groundwater levels in the wetland areas. Additionally, annual average water balance calculations using observed streamflow and precipitation data were used to further constrain simulated ET values. The calibrated steady state water budget corresponded well with the 18 year annual average water budget; precipitation and streamflow were $350,000$ and $158,000 \text{ m}^3 \text{ d}^{-1}$, and $350,000$ and $155,000 \text{ m}^3 \text{ d}^{-1}$ for the simulated and observed values, respectively. The ratio of streamflow to precipitation

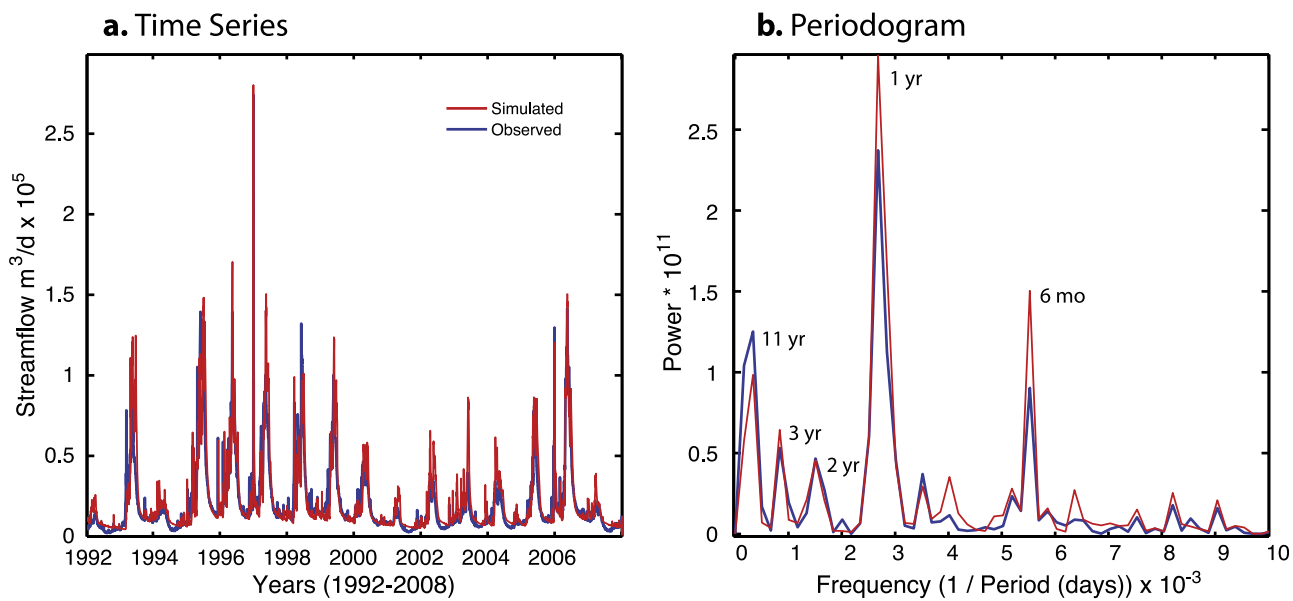


Figure 5. Simulated and observed (a) daily streamflow and (b) periodograms for Incline Creek.

precipitation and groundwater-recharge cycles and associated distributions of residence times of water flowing through the subsurface, effectively resembling the hydraulic memory of the watershed governed by climate, geology, and geomorphology [Smakhtin, 2001]. Periods of wet climate on the order of 2–4 years sustain increases in summertime flow, and seem to contribute to the strong 11 year period in streamflow. It is recognized that the statistical significance of the 11 year cycle in observed and simulated streamflow shown in Figure 5b is low given the limited period of record of only 18 years. However, after analyzing many long-term streamflow records in the region, the 11 year cycle is a common attribute and is statistically significant at the 95% confidence level when tested against red noise [Gilman *et al.*, 1963]. Given that the model produces an 11 year cycle from the input precipitation, suggests that this cycle has significance, even if it is not statistically significant due to the short period of record.

[25] Spatial distributions of groundwater recharge during the winter (Figure 6a), early spring (Figure 6b), and late spring (Figure 6c) indicate that the greatest groundwater-recharge rates occur near stream channels, mountain fronts, and across the alluvial aquifers, where the alluvium is relatively permeable as compared to the upland bedrock areas. Recharge occurs in the upland bedrock areas; however, deep percolation in these areas is restricted by the relatively low vertical hydraulic conductivity of the weathered bedrock. These results are consistent with recent findings from a noble gas and isotopic tracer study of recharge in a nearby high-elevation catchment with similar geology, which suggests that most groundwater recharge to the alluvial aquifer occurs on the lower slopes of the catchment [Singleton and Moran, 2010].

[26] Recharge in the alluvial areas occurs quickly following the onset of snowmelt because of shallow water tables and high rates of deep percolation. Shallow water tables also result in saturated-excess runoff and subsurface

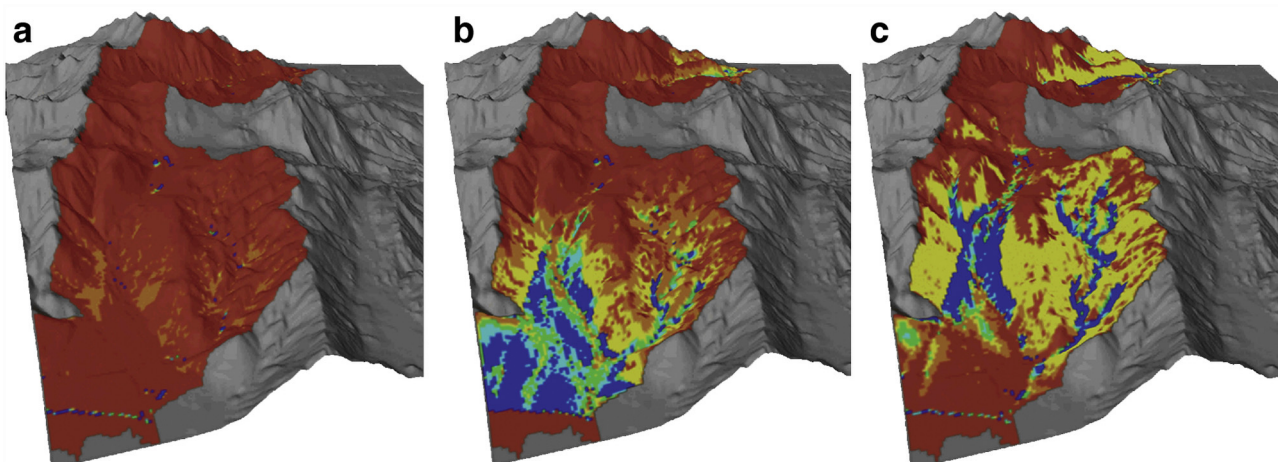


Figure 6. Spatial distributions of groundwater recharge (a) during winter, (b) early spring, and (c) late spring of 2005. Red grid cells indicate negligible recharge, where yellow, green, and blue grid cells indicate low, moderate, and high groundwater recharge, respectively.

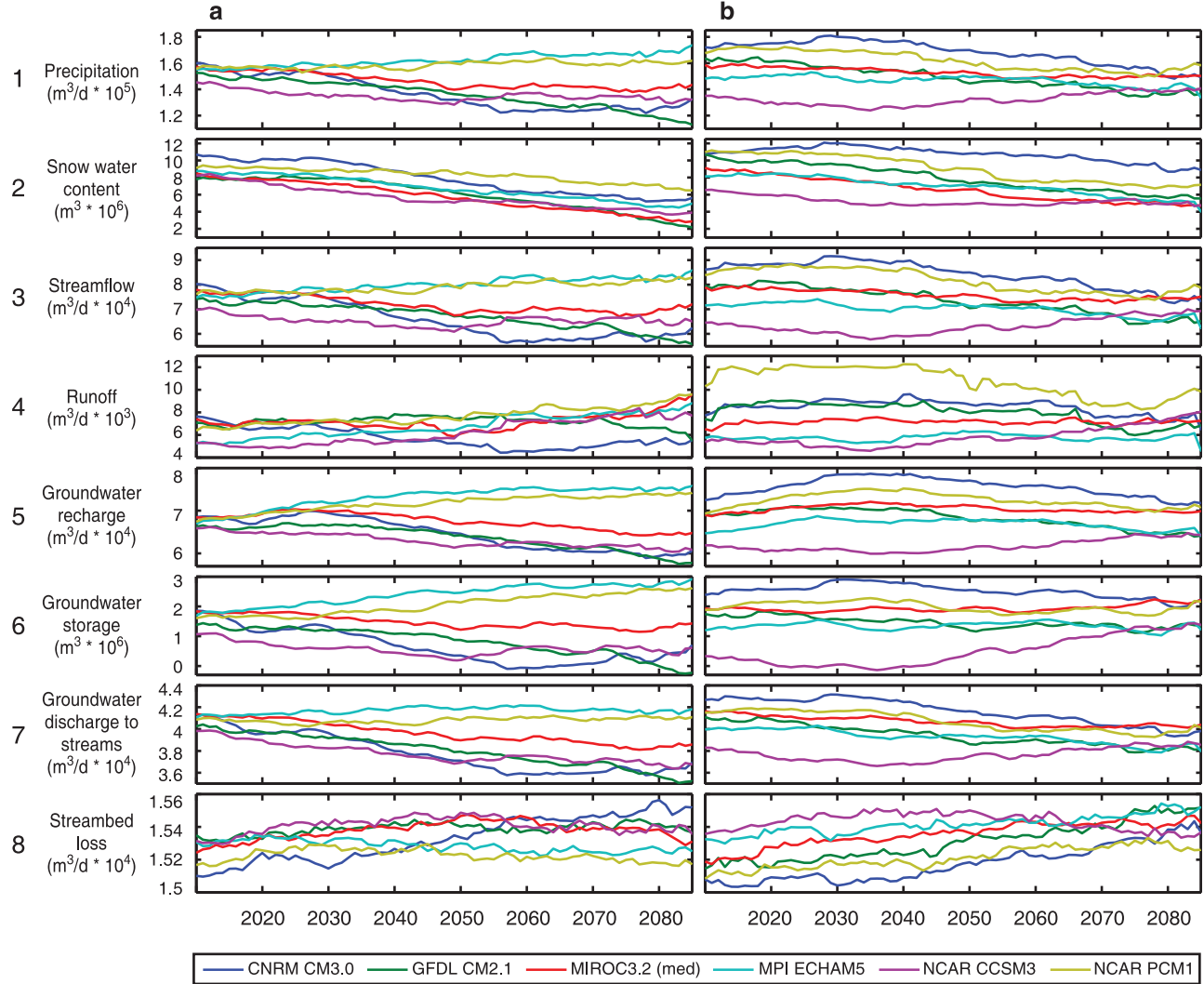


Figure 8. Time series of simulated yearly average hydrologic variables. Simulated hydrologic variables for different GCMs (colored lines) and greenhouse gas emission scenarios (a) A2 and (b) B1. Time series were smoothed using a 30 year moving average. Hydrologic variables included (1) precipitation, (2) snow water content, (3) streamflow, (4) runoff, (5) groundwater recharge, (6) groundwater storage relative to initial conditions, (7) groundwater discharge to streams, and (8) streambed loss.

climate change on surface water and groundwater resources. Long-term simulations are important for these analyses because of the long-term autocorrelation exhibited in hydrologic variables that are related to groundwater storage.

[31] Broadly speaking, results in Figure 8 suggest that changes in annual precipitation drive changes in annual groundwater fluxes; however, seasonal variations in groundwater fluxes are driven by the timing of snowmelt runoff, and more directly by the depth of flow in streams. The effects of increased air temperature on the hydrology of these basins become clear when streamflow components are analyzed on a seasonal basis. To better demonstrate the interplay of seasonal stream gains and losses, Figure 9 illustrates simulations of these variables on a daily basis during a selected 2 year time period (2027–2028) for the CNRM CM3.0 climate model and A2 GHG scenario. The net groundwater discharge to streams is significantly reduced during peak snowmelt runoff due to the bank storage effect [Cooper and Rorabaugh, 1963; Pinder

and Sauer, 1971]. The bank storage effect is important in these watersheds due to rapid runoff and interflow that elevates the stream head more abruptly than the rise in groundwater head near streams. Elevated stream head increases streambed losses to the groundwater and suppresses groundwater discharge to streams, effectively reducing the net groundwater discharge to streams (black line in Figure 9). Earlier snowmelt and streamflow increases the period of time during which groundwater drains to streams, where a longer groundwater-drainage period causes a decrease in July–October streamflow. These results indicate that there is an asymmetric shift toward earlier snowmelt recession that is not completely compensated by earlier onset of snowmelt, thus resulting in a longer period of groundwater drainage to streams during each year.

[32] Figure 10 was developed on the basis of the simulated results, and illustrates our conceptualization of the seasonal drainage of these watersheds. During winter, the snowpack builds, and cold conditions result in negligible

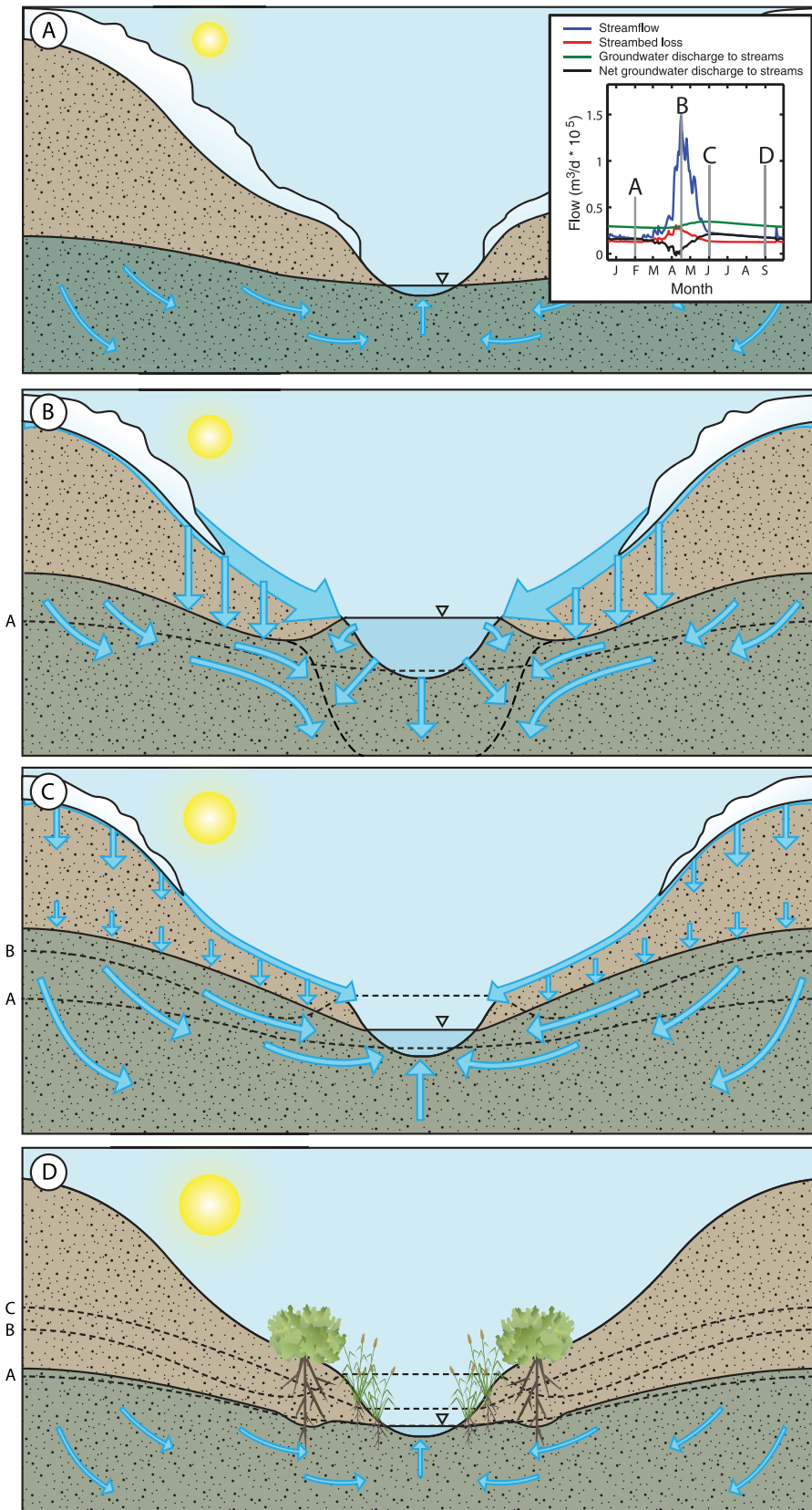


Figure 10. Conceptualization of the seasonal drainage of a snowmelt dominated stream – aquifer system for, (a) early winter with negligible recharge, groundwater storage, and groundwater discharge, (b) spring snowmelt with elevated the stream head, seepage losses to bank storage and shallow aquifers, and suppressed shallow aquifer heads, (c) summer stream recession with peak shallow and regional groundwater discharge to the stream, and (d) late autumn recession of groundwater discharge to the stream.

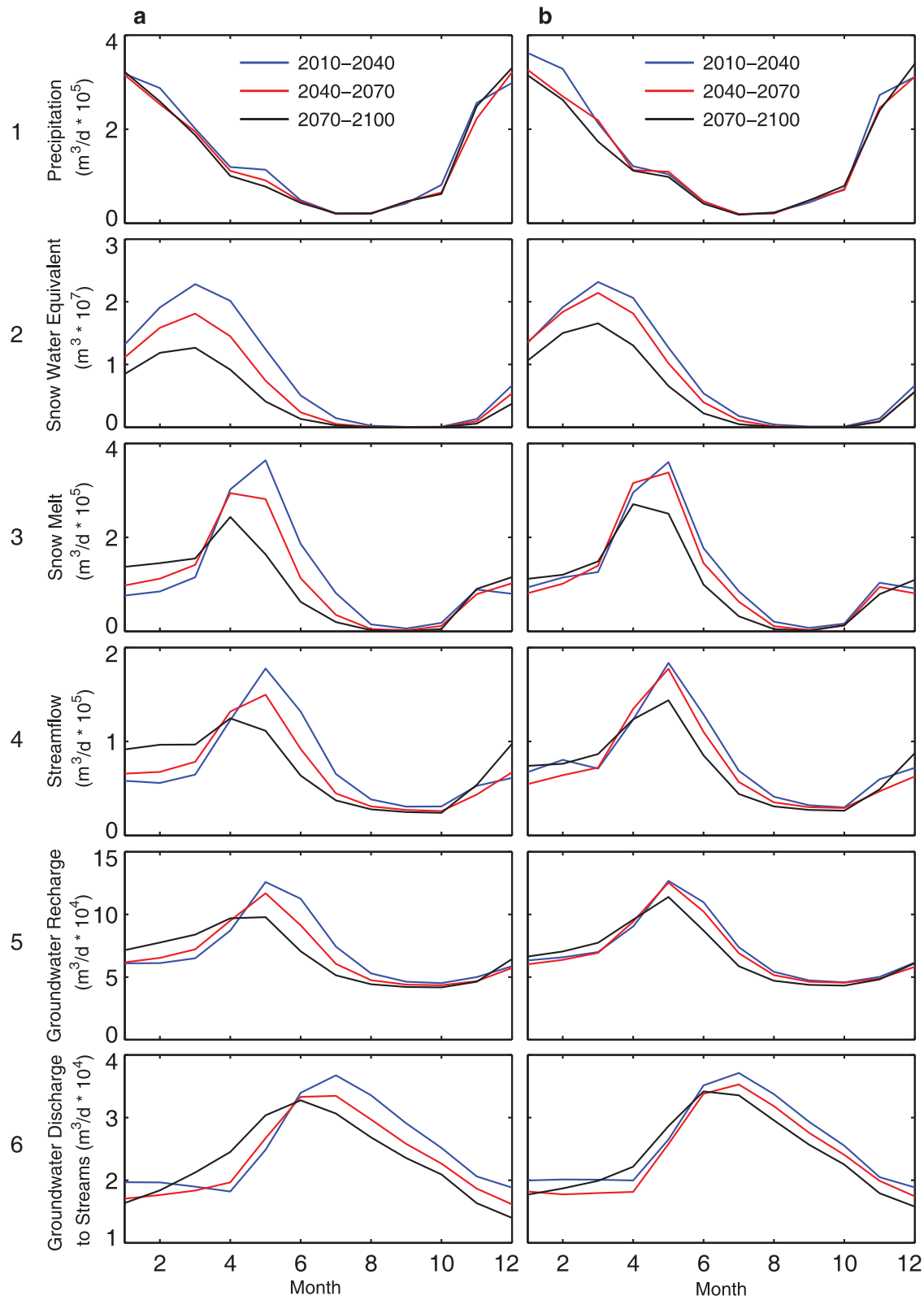


Figure 11. (1) Mean monthly precipitation, (2) snow water equivalent, (3) snow melt, (4) streamflow, (5) groundwater recharge, and (6) groundwater discharge to streams for different time periods and greenhouse gas emission scenarios (a) A2 and (b) B1.

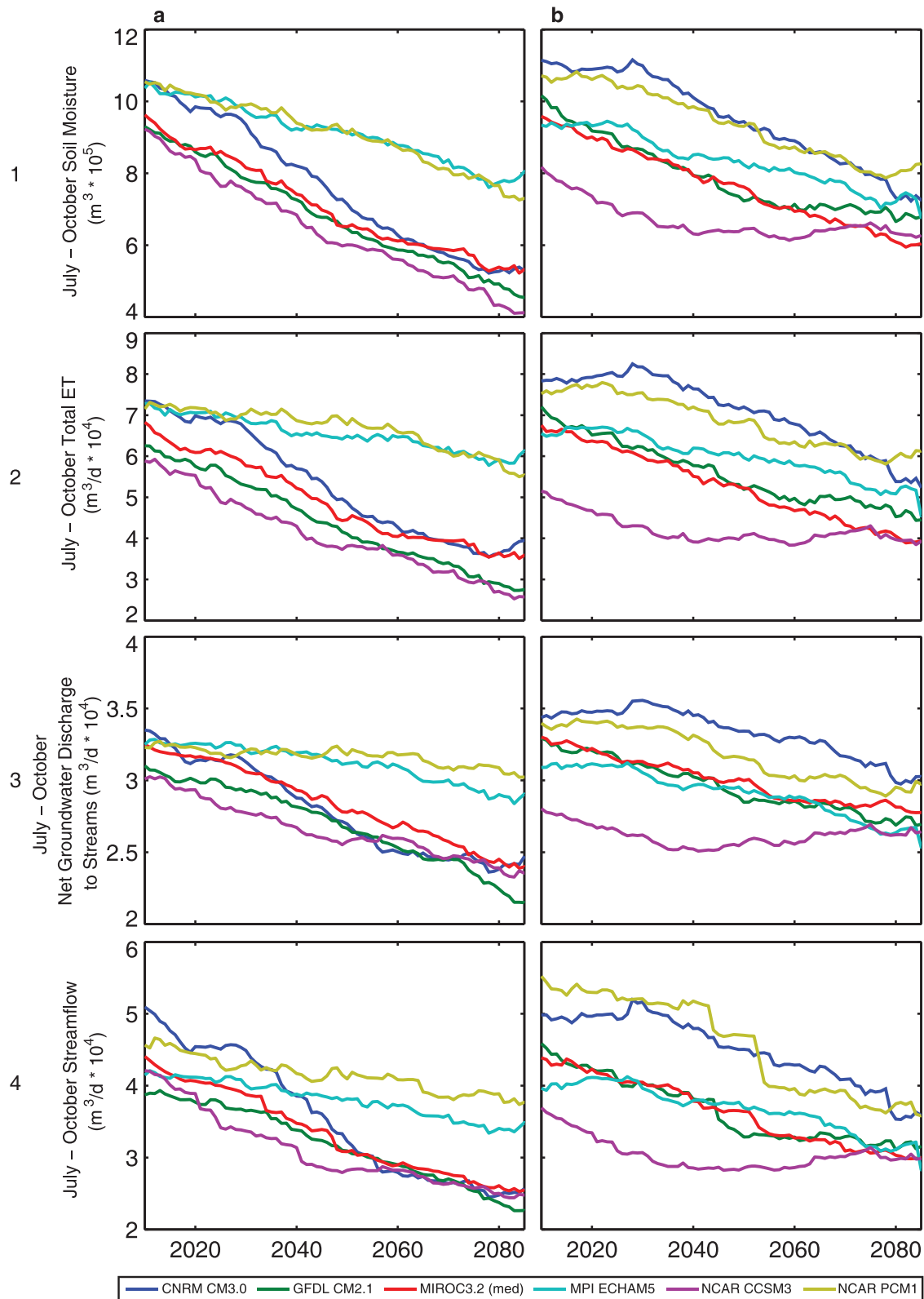


Figure 12. Time series of 30 year moving average July–October (late summer and early autumn) (1) soil moisture, (2) total ET, (3) net groundwater discharge, and (4) streamflow for different GCMs (colored lines) and greenhouse gas emission scenarios (a) A2 and (b) B1. Note the July–October net groundwater discharge and streamflow decreases even if annual precipitation and groundwater recharge increases for GCMs NCAR PCM1 and MPI ECHAM5 (Figures 8).

